Effect of laser linewidths and collisions on resonance fluorescence in a squeezed vacuum

S. Smart and S. Swain
Department of Applied Mathematics and Theoretical Physics, School of Mathematics and Physics, The Queen's University of Belfast, Belfast BT7 1NN, The United Kingdom
(Received 28 October 1991)

We study the system of a single two-level atom interacting with a braodband squeezed vacuum and a classical applied field. The atom is subject to collisions, and the applied field may possess a finite linewidth. The atomic populations, coherences, resonance fluorescence spectrum, and intensity fluctuation spectrum are calculated. Wherever practicable, analytic expressions are obtained that show the dependence of these quantities on the damping parameters. Numerical plots are presented. Two qualitative results that we obtain are the following: (a) we show that the dependence of the populations on the squeezing phase is *increased* by increasing the damping parameters, contrary to what might at first have been expected, and (b) we show that, in the absence of external damping, the squeezing induces strong asymmetries in the off-resonant resonance fluorescence spectra.

PACS number(s): 42.50.Dv, 32.80.−t

I. INTRODUCTION

The interaction of atomic systems with squeezed white noise has been a topic of some interest since Gardiner first pointed out that the two quadratures of the polarization of a two-level atom decay, respectively, faster and slower than the normal decay rate [1]. The next phenomenon to be investigated was resonance fluorescence [2] where it was shown that the relative heights and widths of the Mollow spectrum were strongly phase dependent. In this treatment it was assumed that the classical applied field was monochromatic, and that collisions were negligible. It was also assumed that the squeezed input was a broadband squeezed vacuum. Resonance fluorescence in a narrow-bandwidth squeezed field has been considered by several workers [3], who find that significant narrowing of Rabi peaks and inhibited population decay is possible.

In this paper we consider the effects of finite laser linewidths and collisions on the resonance fluorescence spectrum of a two-level atom in the presence of a broadband squeezed vacuum. We also investigate the atomic populations and calculate the intensity fluctuation spectrum. Two qualitative results that we obtain are (a) that the dependence of the populations on the squeezing phase is increased by increasing the damping parameters, contrary to what might at first have been expected, and (b) that, in the absence of external damping, the squeezing induces strong asymmetries in the off-resonant resonance fluorescence spectra.

Our method of calculation is based upon a diagrammatic analysis of the exact rate equations for the system, which is described in the preceding paper [4]. The starting point for this method is the Gardiner-Collett master equation [5] for a nonequally spaced atomic system interacting with a broadband squeezed vacuum.

II. ATOMIC POPULATIONS

A. The rate equations for a two-level atom in a squeezed vacuum

We consider a two-level atom, with states $|1\rangle$ and $|0\rangle$ and corresponding energies E_1 and E_0 interacting (within the rotating-wave approximation) with a classical field of frequency ω in the presence of a squeezed vacuum [5]. We assume $\hbar=1$. At first we neglect collisions and the laser linewidth, and add in these factors later. In the rate-equation approach, it is convenient to work with the Laplace transform of the probabilities. The equations of motion are found as follows [4]. We consider all possible transitions between the energy eigenstates of the atomic system under investigation, and then write down the rate equations for the atomic populations by inspection. The rate of transitions between a given pair of levels is the sum of a *coherent* rate w due to the applied field and an *incoherent* rate γ due to the squeezed vacuum. For a two-level atom, we have the simple situation shown in Fig. 1. The rate equations are [Eqs. (11) and (12) of Ref. [4]]

$$z\tilde{P}_0-P_0(0)=(\tilde{w}_{10}+\gamma_{10})\tilde{P}_1-(\tilde{w}_{01}+\gamma_{01})\tilde{P}_0+\Delta P_0 , \quad (1)$$

$$z\tilde{P}_1-P_1(0)=(\tilde{w}_{01}+\gamma_{01})\tilde{P}_0-(\tilde{w}_{10}+\gamma_{10})\tilde{P}_1+\Delta P_1 , \quad (2)$$

where the tilde indicates the usual Laplace transform. $P_i(0)$ is the initial occupation probability for state $|i\rangle$ and ΔP_i is defined in Eqs. (15) and (16). For simplicity, we have omitted to write in the Laplace argument z in the $\tilde{P}$'s and $\tilde{w}$'s. $\tilde{w}_{ij}(z)$ is the rate of coherent transitions between atomic levels $|i\rangle$ and $|j\rangle$, and γ_{ij} is the incoherent transition rate between these levels. If we ignore the ΔP_i terms, these equations express (in Laplace space) the fact that the rate of change of the occupation

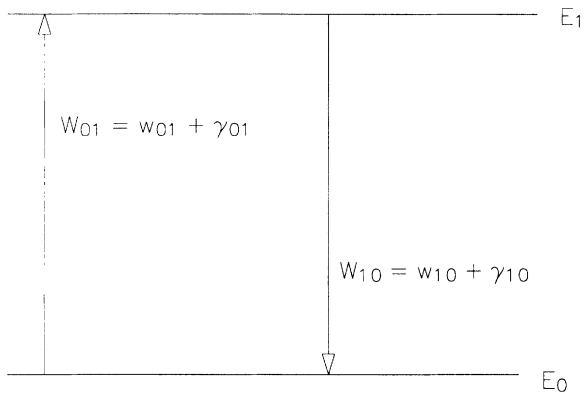

FIG. 1. The coherent and incoherent transition rates in the two-level atom.

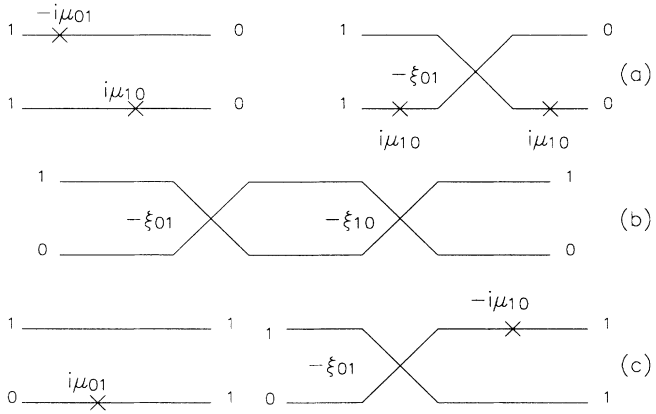

FIG. 2. (a) The diagrams which contribute to the coherent transition rate w_{10}: one lists all the processes that can take one from the density-matrix element ρ_{11} to the element ρ_{00} by means of the dipole (μ) and squeezing (ξ) interactions. The upper line represents the first index of the density matrix and the lower line the second index. (b) The diagrams which contribute to (10). These are the diagrams for remaining in the "state" ρ_{10}. There are two diagrams in this case: the zeroth-order one (not shown) where the system simply remains in this state without any interactions, and the second-order one (illustrated). (c) The diagrams contributing to ΔP_1: one writes down the diagrams which start from any off-diagonal ρ_{ij} and which finish at ρ_{11}. We show the diagrams which start from ρ_{10}; the diagrams starting from ρ_{01} are the mirror images of these.

probability P_i of level $|i\rangle$ (left-hand side) is equal to the difference between the rates of transitions *into* and *out of* that level. For the incoherent transition rates, we have explicitly (cf. Eq. (3) of Ref. [4]),

$$\gamma_{10}=\gamma(N+1),\quad \gamma_{01}=\gamma N\ , \tag{3}$$

where N and $Me^{i\varphi}$ are the squeezing parameters utilized by Collett and Gardiner [5]. (N,M, and φ are real. N and M are zero in the absence of squeezing.) They obey the inequality

$$M^2\le N(N+1)\ . \tag{4}$$

For the coherent rates, squeezing enters through the parameter $\xi_{10}=\gamma M e^{i\varphi}$. We also need the quantities

$$\mu_{10}\equiv|g|e^{i\varphi_L},\quad \Delta=E_{1,0}-\omega_L,\quad \Phi=2\varphi_L-\varphi\ , \tag{5}$$

μ_{10} being the dipole matrix element between levels $|1\rangle$ and $|0\rangle$, φ_L the laser phase, and Δ the detuning. The important phase is Φ, the difference between twice the laser phase and the squeezing phase.

We have described in Sec. III of Ref. [4] a diagrammatic method of calculating the rates $\bar{w}_{ij}$. The dipole interaction causes a transition from state $|1\rangle$ to state $|0\rangle$, measured by the dipole matrix element μ_{10} and the squeezing interaction causes the off-diagonal density-matrix element ρ_{10} to switch to its transpose ρ_{01}, with an amplitude measured by the quantity ξ_{10}. In the diagrams, the dipole interaction is indicated by a cross in the line and the squeezing interaction by an intersection of two lines. For the particular case of a two-level atom, it turns out that the two coherent rates are equal: $\bar{w}_{10}=\bar{w}_{01}\equiv w(z)$. The diagrams for w are obtained by listing all the ways one can proceed from "state" ρ_{11} to state ρ_{00} by means of the two kinds of coherent interaction, dipole and squeezing, as shown in Fig. 2(a). These diagrams correspond to the first and last diagrams of Fig. 4 of Ref. [4]: the other three diagrams in the latter figure do not contribute in the two-level case. For example, if we take a to be the state 1 and b the state 0 in Fig. 2 of [4], we must have $c=1$ in the two-level case. This would give rise to the "diagonal" propagator (11), which is now allowed. Returning now to Fig. 2(a) of this paper, we note that the contribution of the second diagram depends upon the phase Φ. Rules for writing down the contributions of the diagrams are given before Eq. (19) of Ref. [4]. Following this prescription, we obtain

$$w(z)=2\,\mathrm{Re}\left[\frac{|\mu_{10}|^2}{(10)}+\frac{\mu_{10}\xi_{01}\mu_{10}}{(10,01)}\right]\ . \tag{6}$$

The propagators (10) and $(01)_{10}$ are obtained from the diagram of Fig. 2(b) as (in Fig. 2 of Ref. [4] are shown the diagrams for a general propagator (ab); only the third diagram contributes in the two-level situation)

$$(10)=\varepsilon_{10}-\frac{\xi_{01}\xi_{10}}{(01)_{10}},\quad (01)_{10}=\varepsilon_{01} \tag{7}$$

where

$$\varepsilon_{10}=z+i(E_{10}-\omega)+\Gamma_{10}=\varepsilon_{01}^{*} \tag{8}$$

and

$$\Gamma_{10}\equiv\Gamma\equiv(\gamma_{10}+\gamma_{01})/2=\gamma(N+1/2)\ . \tag{9}$$

Γ is associated with the decay of the coherences, whereas γ_{10} and γ_{01} are associated with the decay of the populations. The relationship between the diagonal and off-diagonal decay-rate quantities given in Eq. (9) holds only in the absence of collisions and finite laser linewidths.

These expressions give for $w(z)$,

$$w(z)=\frac{2|g|^2[z+\gamma(N+\frac{1}{2}+M\cos\Phi)]}{[z+\gamma(N+\frac{1}{2})]^2-\gamma^2M^2+\Delta^2}\ . \tag{10}$$

The quantity which determines the steady-state populations is $w(z=0)\equiv w$. In the absence of squeezing ($M=N=0$), the rate equations are unchanged in form but w reduces to

$$w\rightarrow\mathcal{W}\equiv\frac{|g|^2\gamma}{\gamma^2/4+\Delta^2}\ . \tag{11}$$

In the limit of $\gamma\rightarrow 0$, we recover the Fermi golden rule expression

$$\mathcal{W}\rightarrow 2\pi|g|^2\delta(E_{1,0}-\omega_L)\ . \tag{12}$$

Before calculating the populations, we examine the properties of the steady-state coherent rate w. Squeezing drastically alters the value of w. If M is maximal and N is large,

$$M=[N(N+1)]^{1/2}\simeq N+\tfrac{1}{2}-1/(8N) \tag{13}$$

and then

$$w\simeq 2\mathcal{W}[(N+\tfrac{1}{2})(1+\cos\Phi)-\cos\Phi/8N)]\ . \tag{14}$$

For $\Phi=0$, w is strongly enhanced by the squeezing: $w\simeq 4N\mathcal{W}$, whereas for $\Phi=\pi$, w is greatly reduced: $w\simeq\mathcal{W}/4N$. These features are illustrated in Fig. 3, where we have plotted $\ln(w)$. We consider the resonant case, $\Delta=0$, and take $\gamma=1$, $|g|^2=2.5$ (which gives $\mathcal{W}=10$). This shows the increase of w with N for $\Phi\sim 0$ and the decrease for $\Phi\sim\pi$, for N in the range from 0 to 5. Note that w is much more sensitive to small changes in Φ for $\Phi\sim\pi$ than $\Phi\sim 0$.

The quantities ΔP_i (which in general depend upon z) contain all the dependence on the initial values of the off-diagonal density-matrix elements $\rho_{ij}(0)$. In the general case, it is given by Eq. (13) of Ref. [4]. Such terms give rise to transient effects which do not affect the steady state. The diagrams describing these quantities are obtained [4] by considering how one can arrive at the state ρ_{11} by means of the two types of interactions starting from all possible initial coherences ρ_{ij} ($i\neq j$). They are shown in Fig. 3 of Ref. [4] for the general case, but only the first two diagrams, shown here in Fig. 2(c), survive in the two-level case. These diagrams give the contribution

$$\Delta P_1(0)=2\,\mathrm{Re}\left[\frac{-i\mu_{10}\rho_{01}(0)}{(01)}+\frac{i\xi_{01}\mu_{10}\rho_{10}(0)}{(10,01)}\right], \tag{15}$$

$$\Delta P_0(0)=-\Delta P_1(0)\ . \tag{16}$$

The ΔP_i are needed for the calculation of such quantities as the resonance fluorescence spectrum.

The solutions of Eqs. (1) and (2) are

$$\tilde{P}_0(z)=\frac{z\bar{P}_0+w+\gamma_{10}}{z(z+2w+2\Gamma)}\ , \tag{17}$$

$$\tilde{P}_1(z)=\frac{z\bar{P}_1+w+\gamma_{01}}{z(z+2w+2\Gamma)}\ , \tag{18}$$

where $\bar{P}_i\equiv P_i(0)+\Delta P_i$ and Γ is defined in Eq. (9). For the steady-state solution we obtain

$$P_1(\infty)=\lim_{z\rightarrow 0}z\tilde{P}_1(z)=\frac{1}{2}\frac{\gamma N+w}{\gamma N+w+\gamma/2}\ , \tag{19}$$

which agrees (after a change of notation) with the expression obtained in Ref. [2]. From this formula, we see that $P_1(\infty)$ will approach its asymptotic value of $\frac{1}{2}$, no matter what the value of Φ, if $\gamma N+w\gg\gamma/2$. That is, if either $N\gg 1$ or $|g|^2\gg N\gamma^2/8$ (the latter expression assuming that $N\gtrsim 1$). These two inequalities correspond to saturation by the squeezing field or the dipole field, respectively.

The important quantity is $\gamma N+w$. For phase-dependent effects to be noticeable we must have $w\geq\gamma N$; that is, the coherent rate must dominate the incoherent rates due to squeezing. We must also be well away from saturation.

These features are clearly seen in Fig. 4, where we plot P_1, again taking $\Delta=0$, $\gamma=1$, and $|g|^2=2.5$. It can be seen that the P_1 graphs have the same qualitative features as the w graphs, with the difference that the P_1 curves saturate to a constant value with N. (For $\Phi\sim\pi$, this occurs at much larger values of N than those shown in Fig. 4.) In the absence of squeezing, the applied classical field would produce a steady-state value of P_1 of about 0.476. The particularly interesting feature is that for $\Phi\gtrsim 3\pi/4$, $P_1(\infty)$ decreases at first from this value as the squeezing is increased. This is due to the decrease in the value of w, which in turn may be considered due to the interference between the two diagrams in Fig. 2(a) being destructive for $\varphi\sim\pi$. However, for N sufficiently large, the incoherent rates γN begin to dominate the coherent rate w, and $P_1(\infty)$ begins to increase. Thus the behavior of $P_1(\infty)$—its rapid increase with N for small values of Φ, and for $\Phi\sim\pi$, its fall to a minimum followed by a steady rise—may be understood in terms of the behavior of the coherent and incoherent transition rates.

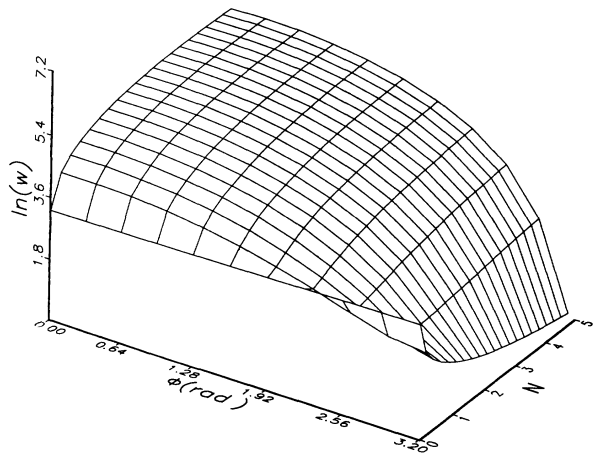

FIG. 3. The natural logarithm of the coherent transition rate $\bar{w}_{10}(0)\equiv w$ as a function of the squeezing phase Φ and the amplitude N.

B. Inclusion of collisions and laser linewidths

Since this rate-equation approach is based on the master equation, it is a relatively easy matter to include other damping mechanisms, such as collisions [6]. In the *pro-*

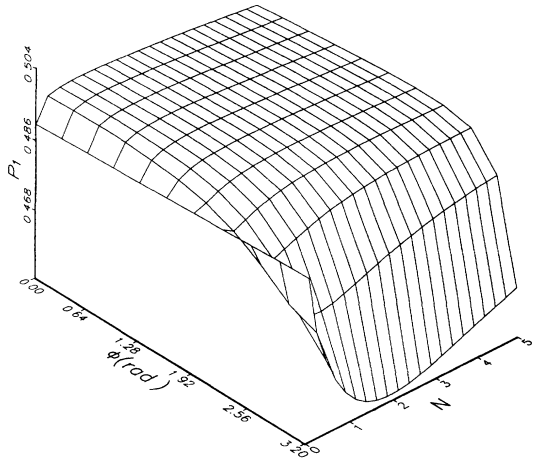

FIG. 4. The steady-state occupation probability $P_1(\infty)$ as a function of the squeezing phase Φ and the amplitude N.

duction of squeezed light, one would expect such effects to greatly reduce the degree of squeezing attainable. In the *interaction* of squeezed light with atomic systems, it is of considerable interest to see how they affect the phase dependence. We consider first the effect of collisions. If Q_i is the rate of inelastic collisions and Q_e is the rate of elastic collisions, their effect on resonance fluorescence may be taken into account by making the replacements

$$\gamma_{10}\rightarrow\gamma_{10}+Q_i,\quad \gamma_{01}\rightarrow\gamma_{01}+Q_i\ , \tag{20}$$

$$\Gamma\rightarrow\Gamma+Q\quad \text{where} Q=(Q_i+Q_e)/2\ . \tag{21}$$

We have also shown how to take into account the effects of finite laser linewidths when this is due to phase diffusion [7]. In that paper we assumed a quantum treatment of the applied field. We proceed in the present semiclassical treatment by analogy with the quantum case. It is found that the effects of a finite-phase diffusion linewidth L may be taken into account by adding this quantity to the expression (9) for Γ. The result is that w is modified to

$$w=\frac{2|g|^2(\chi+\gamma M\cos\Phi)}{\chi^2+\Delta^2-\gamma^2M^2}\ , \tag{22}$$

where

$$\chi=\gamma(N+\tfrac{1}{2})+Q+L\ . \tag{23}$$

As may have been anticipated, the parameters describing collisions and laser linewidth add to the incoherent decay rates due to squeezing and spontaneous emission. The effect of the additional damping terms is to reduce the absolute value of w, and thus the value of $P_1(\infty)$. However, these damping terms also introduce a qualitative change in the behavior of w for $\Phi\sim 0$. For large values of N, w does not increase linearly with N, but saturates to a constant value. This is illustrated in Fig. 5. (Here we make a linear plot of w, rather than a logarithmic plot as in Fig. 3.) The rather surprising result of this is to greatly *increase* the sensitivity of $P_1(\infty)$ to changes in the phase Φ. Thus in Fig. 6 we see that in the absence of these additional damping parameters, the net change in P_1 due to changes in Φ is about 10%, whereas with $L=Q=1$, the net change is of order 33%. With the increase in these damping parameters, the region of maximum sensitivity to Φ tends to smaller values of N.

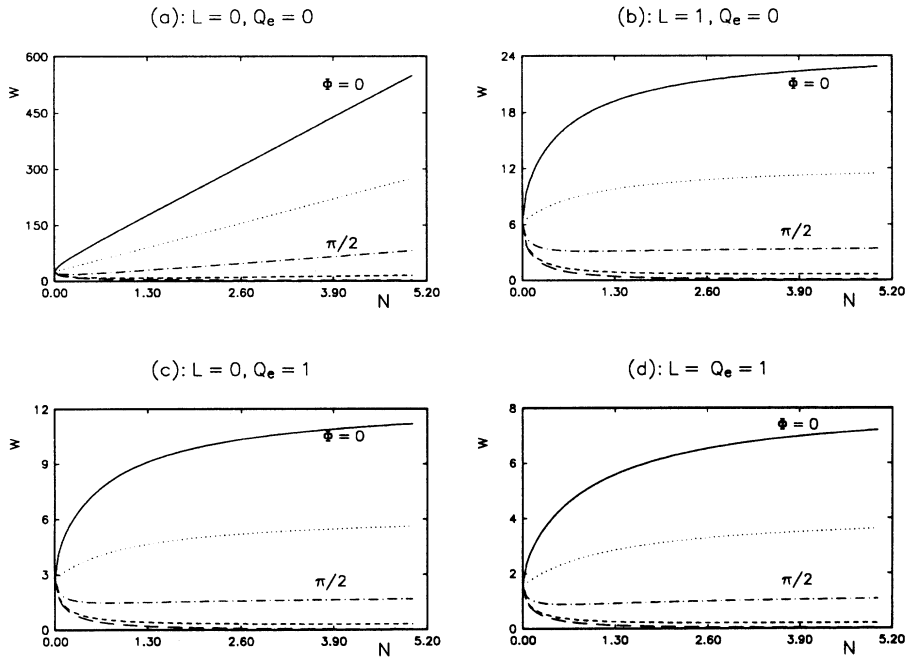

FIG. 5. The coherent rate w as a function of N for $\Phi=0$, $\pi/4$, $\pi/2$, $3\pi/4$, and π, $\Phi=0$ being the top graph and $\Phi=\pi$ the bottom, for different values of the laser linewidth and collision parameters.

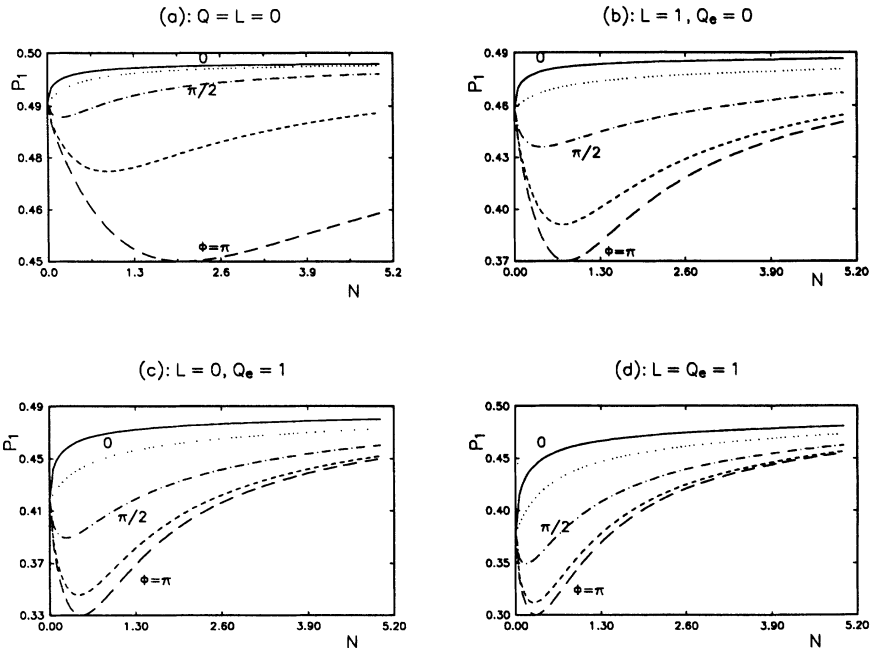

FIG. 6. The excited-state population $P_1(\infty)$ as a function of N for $\Phi=0$, $\pi/4$, $\pi/2$, $3\pi/4$ and π, for different values of the laser linewidth and collision parameters.

III. RESONANCE FLUORESCENCE

A. Off-diagonal density-matrix elements

In order to discuss resonance fluorescence we need the steady-state off-diagonal elements of the density matrix. They may be calculated in the present approach by substituting in Eq. (15) of Ref. [4] the diagonal matrix elements (populations) obtained from a solution of the rate equations. For a two-level system, this equation reduces to

$$\tilde{\sigma}_{10}(z)=\frac{B_{10}}{(10)}\frac{B_{01}\xi_{10}}{(10,01)}\ , \tag{24}$$

where $\sigma_{10}(t)\equiv\rho_{10}(t)\exp(i\omega_{10}t)$ and the B_{ij} depend upon the diagonal elements

$$B_{10}=\rho_{10}(0)-i\mu_{10}[\tilde{P}_0(z)-\tilde{P}_1(z)]\ , \tag{25a}$$

$$B_{01}=\rho_{01}(0)+i\mu_{01}[\tilde{P}_0(z)-\tilde{P}_1(z)]\ . \tag{25b}$$

Hence for the steady state we obtain

$$\sigma_{01}(\infty)=\frac{i\mu_{01}\gamma[(\chi+i\Delta)+\gamma Me^{i\Phi}]}{[\gamma_{01}+\gamma_{10}+2Q_i+2w](\chi^2+\Delta^2-\gamma^2M^2)}\ , \tag{26}$$

with w given by Eq. (22).

If we neglect collisions and laser linewidth, set the amplitude of the external field, Δ and φ to zero, and assume $\rho_{10}(0)=\alpha+i\beta$, we find from Eq. (24) that

$$\sigma_{10}(z)=\frac{\alpha(z+\Gamma-\gamma M)+i\beta(z+\Gamma+\gamma M)}{(z+\Gamma-\gamma M)(z+\Gamma+\gamma M)}\ , \tag{27}$$

from which we recover Gardiner's result that the real and imaginary parts of the coherence decay at the rates $\Gamma\pm\gamma M$, respectively [1].

B. The resonance fluorescence spectrum

The spectrum in resonance fluorescence is usually calculated by means of the quantum regression theorem, which effectively makes use of the solutions for the off-diagonal elements of the density matrix. We largely follow the approach presented in Ref. [6], which includes the effect of collisions and laser linewidths, and where the details may be found.

The quantum regression theorem requires us to find the quantity $\tilde{\Lambda}_{10}(z)$, where $\tilde{\Lambda}$ is defined to satisfy the same equation of motion as the density matrix ρ but with the different initial conditions [6]

$$\begin{aligned}&\Lambda_{11}(0)=\Lambda_{01}(0)=0\ ,\\ &\Lambda_{10}(0)=\rho_{11}(\infty)\ ,\\ &\Lambda_{00}(0)=\sigma_{01}(\infty)\ .\end{aligned} \tag{28}$$

The quantities $\rho_{11}(\infty)$ and $\sigma_{01}(\infty)$ are the steady-state solutions of the density-matrix equations, given in Eqs. (18) and (26). From Eq. (24) we have

$$\tilde{\Lambda}_{10}(z)=\frac{B_{10}}{(10)}-\frac{B_{01}\xi_{10}}{(10,01)}\ , \tag{29}$$

where now

$$B_{10}=\rho_{11}(\infty)-i\mu_{10}[\tilde{\Lambda}_{00}(z)-\tilde{\Lambda}_{11}(z)]\ , \tag{30}$$

$$B_{01}=i\mu_{01}[\tilde{\Lambda}_{00}(z)-\tilde{\Lambda}_{11}(z)]\ . \tag{31}$$

The $\tilde{\Lambda}_{ii}(z)$ may be found from Eqs. (17) and (18), where the "initial values," $\bar{\Lambda}_{ij}\equiv\Lambda_{ij}(0)+\Delta\Lambda_{ij}$, obtained using

Eq. (15), are given by

$$\bar{\Lambda}_{11}=\frac{i\mu_{01}\rho_{11}(\infty)}{(10)}+\frac{i\mu_{10}\xi_{01}\rho_{11}(\infty)}{(10,01)}\ , \tag{32}$$

$$\bar{\Lambda}_{00}=\sigma_{01}(\infty)-\bar{\Lambda}_{11}(0)\ . \tag{33}$$

We find

$$\Lambda_{10}(z)=\frac{(z+L)[\Omega^2/2+(z+L+2\Gamma+2Q_i)\varepsilon_{01}]\rho_{11}(\infty)-i\mu_{10}(z+\gamma+L)(\varepsilon_{01}+\gamma Me^{-i\Phi})\sigma_{01}(\infty)}{(z+L)[\Omega^2(z+\chi+L+\gamma M\cos\Phi)+(z+2\Gamma+2Q_i+L)(\varepsilon_{10}\varepsilon_{01}-\gamma^2M^2)]}\ , \tag{34}$$

where now $\varepsilon_{10}=z+i(E_{10}-\omega)+\chi-L$ and $\varepsilon_{01}=z-i(E_{10}-\omega)+\chi+3L$ in order to take into account collisions and laser linewidths, and $\Omega\equiv 2|g|$ is the Rabi frequency.

The resonance fluorescence spectrum $g(\omega)$ is obtained from the relationship [6]

$$g(\omega)=2\,\mathrm{Re}\Lambda_{10}[z=-i(\omega-\omega_{10})]\ . \tag{35}$$

In general, we have to evaluate this expression numerically. However, if $|g|$ greatly exceeds the damping parameters, we may obtain approximate analytic expressions. Assuming zero detuning for simplicity, and restricting ourselves to the two extreme values of the phase ($\Phi=0$ or π), we find

$$g(\omega)=\frac{AL}{\omega^2+L^2}+\frac{(\frac{1}{2}-A)(a+L)}{\omega^2+(a+L)^2}+\frac{\hat{\Gamma}/4}{(\omega+\Omega)^2+\hat{\Gamma}^2}+\frac{\hat{\Gamma}/4}{(\omega-\Omega)^2+\hat{\Gamma}^2}\ , \tag{36}$$

with

$$a=\gamma(N+\tfrac{1}{2}\pm M)+Q+L \rightarrow\gamma(N+\tfrac{1}{2}\pm M)\ , \tag{37}$$

$$\hat{\Gamma}=\{\gamma[3(N+\tfrac{1}{2})\mp M]+3L+Q+2Q_i\}/2 \rightarrow\gamma[3(N+\tfrac{1}{2})\mp M]/2\ , \tag{38}$$

$$A=[L(2\Gamma+2Q_i+L)(2\Gamma+2Q+8L)+\gamma(\gamma+L)(a+3L)-L\hat{\Gamma}(\hat{\Gamma}+a+L)]/(2\Omega^2a) \rightarrow\gamma^2/2\Omega^2\ . \tag{39}$$

Where there are double signs, the upper refers to the case $\Phi=0$ and the lower to $\Phi=\pi$. The limits are those that are obtained when squeezing is the only source of damping (no collusion or linewdiths). Since $A\sim 1/\Omega^2$, it is consistent with our approximations to replace it by zero. However, we have retained it here to show the presence of the "coherent" contribution to the spectrum, which is centered on the applied field frequency ω_{10} [the first term in Eq. (36)]. The width of this contribution is equal to the linewidth of the applied field, and is independent of the squeezing. Its intensity is but weakly dependent on the squeezing. In the opposite limit to that considered here, the weak-field limit [2], it is found by contrast that its intensity does depend strongly on the squeezing.

The remaining terms in Eq. (36) represent the incoherent contribution to the spectrum. In consists of three Lorentzian peaks, centered on $\omega=0$ and $\pm\Omega$. The heights and widths of these peaks depend strongly on the squeezing, *provided* the laser width and collisional damping is small.

C. Numerical results for the resonance fluorescence spectrum

In Fig. 7 we put the collisional and linewidth parameters equal to zero and consider numerically the effects of detuning on the resonance fluorescence spectrum. All quantities are measured in units of γ, and we assume a Rabi frequency of 10 throughout. In this figure we have omitted the coherent contributions. Figure 7(a) shows the situation where the detuning $\Delta\equiv E_{1,0}-\omega=1$, a modest value. For $N=0$ the spectrum is, as is well known, symmetric, irrespective of the value of the detuning. However, as N increases, the high-frequency side peak grows in amplitude at first whilst the low-frequency side peak decreases. The result is that for $N=0.2$, for example, the spectrum is markedly asymmetric. Eventually, the high-frequency side peak also begins to decline, but a significant asymmetry remains. Another feature is that the central peak rapidly declines in amplitude as N increases. These effects are accentuated for larger detunings, as shown in Fig. 7(b) where $\Delta=10$. For the case $\Phi=\pi$, we also find similar asymmetries. However, these features are rather obscured in Figs. 7(c) and 7(d) by the influence of the central peak, which for $\Delta=1$ grows very rapidly with N at first, and then undergoes a slow decline. For $\Delta=10$, the central peak is not so dominant as in the $\Delta=1$ case. It is always more important in the $\Phi=\pi$ situation than the $\Phi=0$ case.

The effect of introducing laser linewidths and collisions is qualitatively similar to the zero detuning case which we discuss in the next paragraph. Here we point out that these factors too can introduce asymmetries in the off-resonant resonance fluorescence spectrum. These asymmetries, however, are present when N is zero, and so can be distinguished from those induced by the squeezing.

In the next two figures we present the incoherent resonance fluorescence spectrum for resonant excitation ($\Delta=0$) and consider the effect of introducing collisions and linewidths. We first consider the case $\Phi=0$. For comparison, Fig. 8(a) shows the spectrum when the laser linewidth is zero and there are no collisions. We take $\Omega=10$, and N varies from 0 to 0.30 in steps of 0.06. As before, all quantities are measured in units of $\gamma(\gamma=1)$, and throughout we assume $|M|=[N(N+1)]^{1/2}$. In Fig.

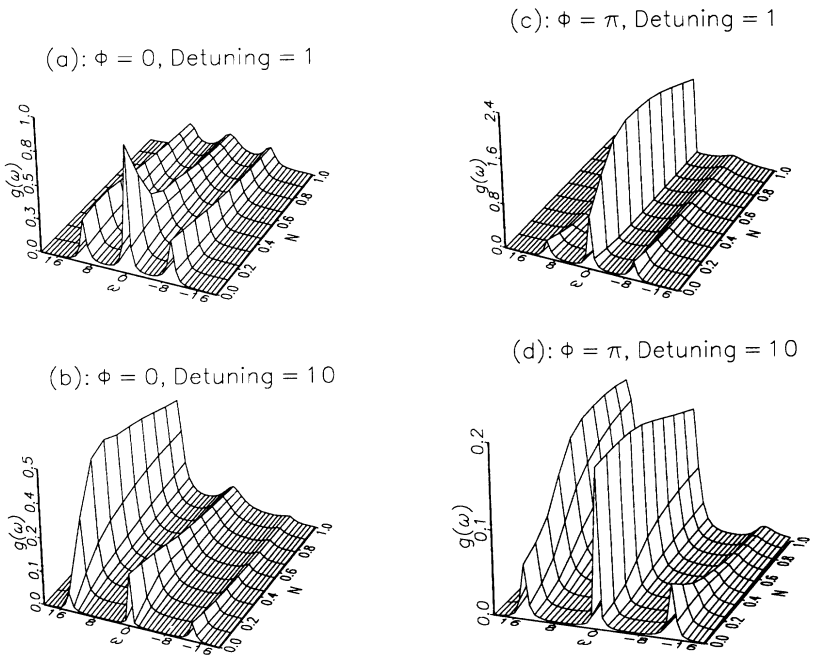

FIG. 7. The resonance fluorescence spectrum for off-resonant excitation without laser linewidth and collision effects.

8(b) we show the effects of laser linewidths ($L=1$, $Q_e=Q_i=0$), in Fig. 8(c) the effect of inelastic collisions ($Q_i=1$, $L=Q_e=0$), and in Fig. 8(d) the effect of elastic collisions ($Q_e=1$, $L=Q_i=0$). In all cases, it is clear that marked changes in the spectrum occur even for small values of N: the height of the central peak drops rapidly as N increases, whereas the heights of the side peaks vary hardly at all, and for $N \gtrsim 0.5$ (not shown) the three peaks are almost equal in intensity. Laser linewidths are seen to have the greatest effect in reducing the overall height of the spectrum, and in broadening all three peaks. With collisions, the central peak height is not strongly dependent on the type of collision, but the side peaks are much reduced in height and increased in width for the inelastic case as compared with elastic collisions. It is clear that relatively small values of these external damping parameters significantly reduce the distinctive properties of the spectrum introduced by squeezing. The relative heights and widths of the peaks are given approximately by expressions (36)–(39).

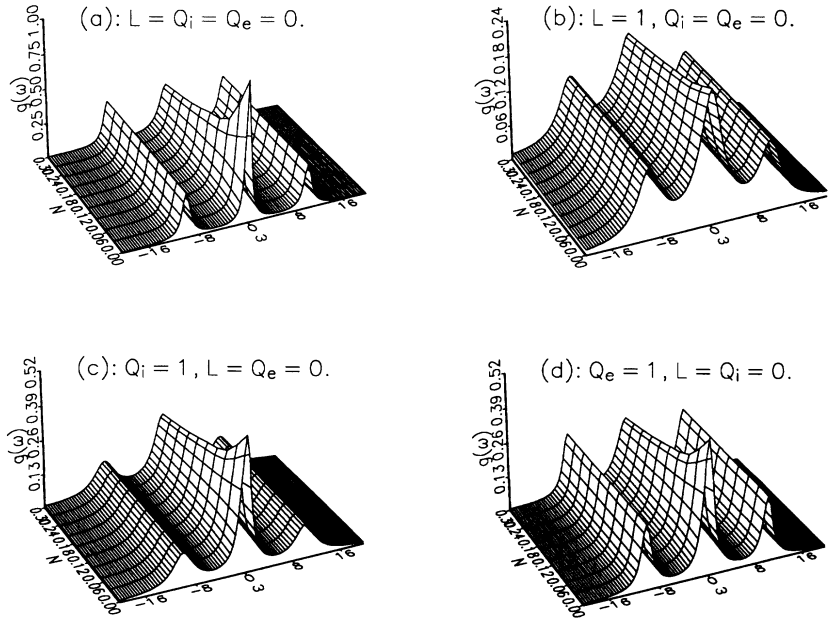

FIG. 8. The resonance fluorescence spectrum for resonant excitation with laser linewidth and collision effects. The squeezing phase Φ is zero.

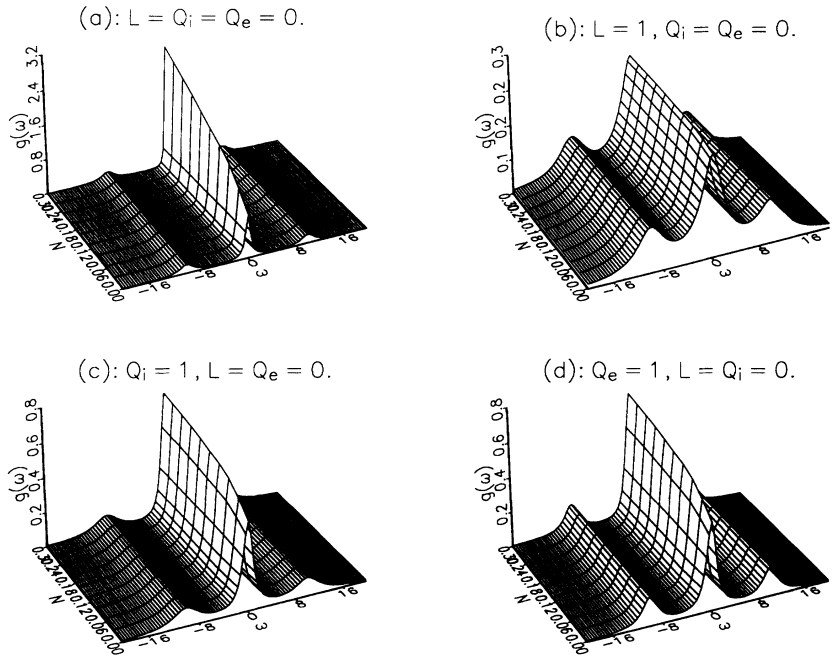

FIG. 9. The resonance fluorescence spectrum for resonant excitation with laser linewidth and collision effects. The squeezing phase $\Phi=\pi$.

Figure 9 has the same parameter values as Fig. 8 except that now we take $\Phi=\pi$. The most obvious difference between these figures is the fact that the central peak increases strongly in height as N increases for the $\Phi=\pi$ case, particularly for zero external damping. The general effect of the external damping is similar, independent of the value of the phase.

D. The intensity fluctuation spectrum

The intensity correlation function $g^{(2)}(\tau)$ has been calculated recently for the case of radiative damping only by D'Souza, Jayarao, and Lawande [8]. Here we use a similar method to that of Sec. III C, referring to Ref. [6] for details. In the case of zero detuning, it is possible to calculate the spectrum exactly. $g^{(2)}(\tau)$ is equal to $\Pi_{11}(\tau)$, where the quantity Π obeys the same equation of motion as ρ (if $L=0$) but with the initial conditions

$$\Pi_{11}(0)=\Pi_{10}(0)=\Pi_{01}(0)=0, \quad \Pi_{00}(0)=\rho_{11}(\infty) . \tag{40}$$

For resonant excitation we find

$$g^{(2)}(\tau)=[\rho_1(\infty)]^2\left[1-\frac{e^{-(2\Gamma+2Q_i+\chi\mp\gamma M)t/2}}{\Omega'[(\gamma N+Q_i)(\chi\mp\gamma M)+\Omega^2/2]}\right.$$
$$\times\left.\left[\Omega'[(\gamma N+Q_i)(\chi\mp M)+\Omega^2/2]\cos(\Omega' t)+\frac{1}{4}[\Omega^2(2\Gamma+2Q_i+\chi\mp\gamma M)]\right.\right.$$
$$\left.\left.+2\{(\gamma N+Q_i)[(\chi\mp\gamma M)(\chi\mp\gamma M-2\Gamma-2Q_i)-2\Omega^2]\}\sin(\Omega' t)\right]\right] , \tag{41}$$

where

$$\Omega'^2=\Omega^2-(2\Gamma+2Q_i-\chi\pm\gamma M)^2/4 \tag{42}$$

and the upper sign refers to the $\Phi=0$ case, the lower to the $\Phi=\pi$. We would not expect a marked dependence of the spectra of Φ because of the form of the exponent in Eq. (41). An interesting feature of these results is that there is a value of the squeezing parameter N that makes the effective Rabi frequency Ω' disappear, if we take the upper sign in (42). This occurs at

$$N=(b-1/2)^2/2b , \tag{43}$$

where $b\equiv(2\Omega-2Q_i+Q+L)/\gamma$. Then $g^{(2)}(\tau)$ is governed by a simple exponential behavior,

$$g^{(2)}(\tau)=[\rho_{11}(\infty)]^2(1-e^{-(2\Gamma+2Q_i+\chi-\gamma M)t/2}) , \tag{44}$$

showing a monotonic increase to its steady-state value.

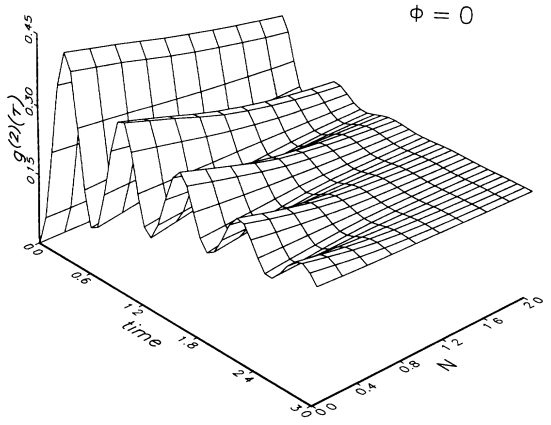

FIG. 10. The intensity fluctuation spectrum for resonant excitation in the absence of laser linewidth and collision effects ($L=Q=0$). The squeezing phase Φ is zero.

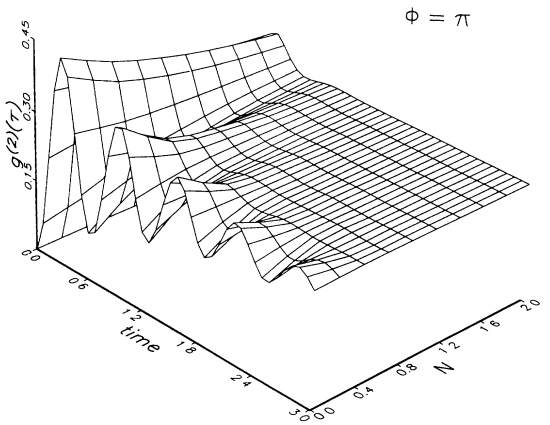

FIG. 11. The intensity fluctuation spectrum for resonant excitation in the absence of laser linewidth and collision effects ($L=Q=0$) with $\Phi=\pi$.

E. Numerical results for the intensity fluctuation spectrum

In general, the exponential term cause the Rabi oscillations to decay away rapidly, whatever the value of Φ, even for small values of N. This is illustrated in Figs. 10 and 11. In these figures we have taken $\Omega=10\gamma$ as before. Here we have set $L=Q_i=Q_e=0$. The effect of choosing nonzero values for these parameters is to wash out the Rabi oscillations in a qualitatively predictable way.

IV. CONCLUSIONS

We have investigated the interaction of a two-level system with a broadband squeezed vacuum in the presence of an external classical field. We have introduced additional damping processes, namely those due to the applied field possessing a finite linewidth, and the atom being subject to elastic or inelastic collisions. Analytic expressions have been obtained for the atomic populations, coherences, resonance fluorescence spectrum, and intensity fluctuation spectrum, showing explicitly the effects of laser linewidths and collisions. Results that we have obtained include the following: (i) the fact that the sensitivity of the atomic populations to the squeezing phase can be *increased* greatly by introducing these damping processes, and (ii) in the absence of these damping processes, strong asymmetries may be introduced into the *off-resonant* resonance fluorescence spectrum by the squeezing process. (In the absence of squeezing and additional damping, the resonance fluorescence spectrum is always symmetric, whatever the value of the detuning.)

ACKNOWLEDGMENTS

This work was supported by the United Kingdom Science and Engineering Research Council. In addition, S. Smart wishes to thank the Department of Education for Northern Ireland for financial support.

[1] C. W. Gardiner, Phys. Rev. Lett. **56**, 1917 (1986).
[2] H. J. Carmichael, A. S. Lane, and D. F. Walls, J. Mod. Opt. **34**, 821 (1987); Phys. Rev. Lett. **58**, 2539 (1987).
[3] A. S. Parkins and C. W. Gardiner, Phys. Rev. A **37**, 3867 (1988); H. Ritsch and P. Zoller, *ibid.* **38**, 4657 (1990); A. S. Parkins, *ibid.* **42**, 4352 (1990).
[4] S. Smart and S. Swain, the preceding paper, Phys. Rev. A **44**, 6857 (1992).
[5] C. W. Gardiner and M. J. Collett, Phys. Rev. A **31**, 3761 (1985).
[6] S. Swain, Adv. At. Mol. Phys. **16**, 159 (1980).
[7] K. I. Osman and S. Swain, J. Phys. B **13**, 2375 (1980).
[8] R. D'Souza, A. S. Jayarao, and S. V. Lawande, Phys. Rev. A **41**, 4083 (1990).

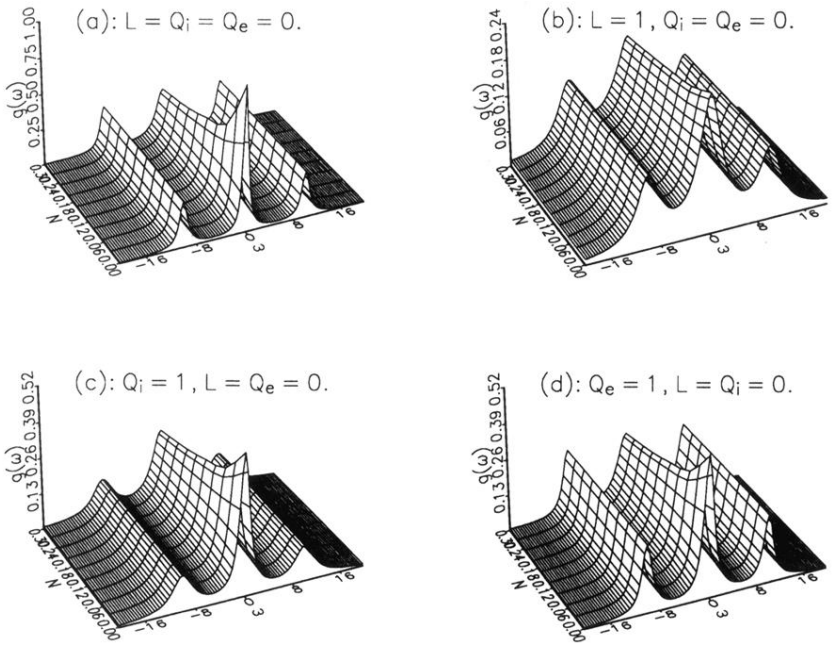

FIG. 8. The resonance fluorescence spectrum for resonant excitation with laser linewidth and collision effects. The squeezing phase Φ is zero.

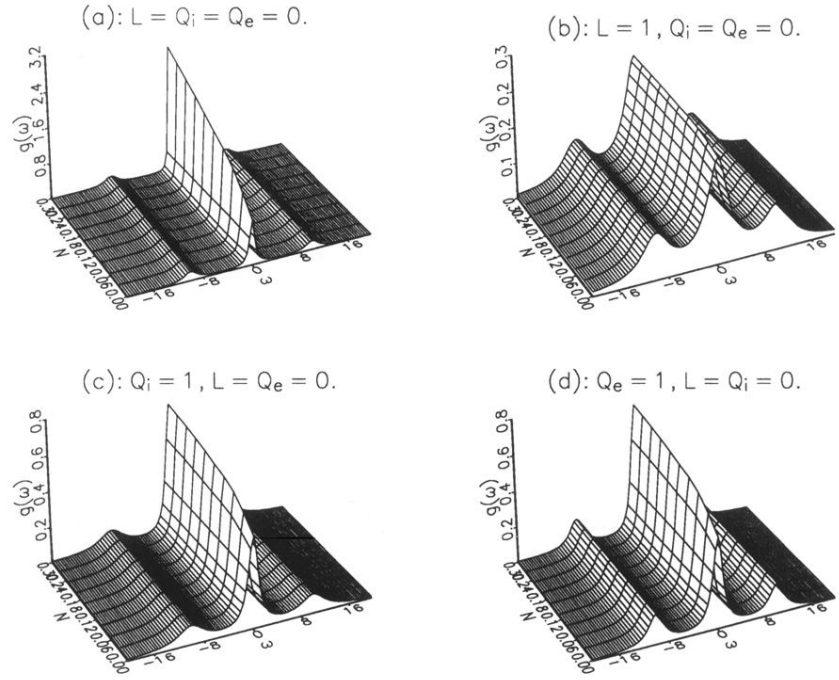

FIG. 9. The resonance fluorescence spectrum for resonant excitation with laser linewidth and collision effects. The squeezing phase $\Phi=\pi$.